# *Ultra-broadband antenna with robustness to body detuning for 4G eyewear devices*

# Ultra-Broadband Antenna with Robustness to Body Detuning for 4G Eyewear Devices

Aykut Cihangir, Chinthana J. Panagamuwa, *Member, IEEE*, William G. Whittow, *Senior Member, IEEE*, Frédéric Gianesello, *Member, IEEE*, Cyril Luxey, *Senior Member, IEEE*

***Abstract*—An ultra-broadband antenna design for 4G cellular coverage in eyewear devices is presented in this paper. The antenna has been designed considering a realistic eyewear PCB and its dielectric frame. In order to overcome any negative effects from the antenna's surroundings (frequency detuning due to the head and the hand of the user), the antenna was designed to cover continuously the 700-2700 MHz band with a reflection coefficient below -6 dB instead of a dual-band behavior usually required for 4G operation: 700-960 MHz and 1700-2700 MHz. The antenna was of capacitive coupling element type with its appropriate matching network to cover the mentioned frequency interval. To emulate a realistic device, an ABS plastic dielectric frame was manufactured using 3D-printing technology. The antenna was simulated and tested in three different use-cases as: "default case with user's head", "with head and hand" and "free space" cases. State-of-the art performance is demonstrated. The specific absorption rate (SAR) behavior was also investigated through simulations and measurements to check the compliance with regulations.**

***Index Terms*—eyewear, electrically small antennas, coupling element, matching network, detuning, 4G, LTE.**

## I. Introduction

Wearable technology devices have gained considerable popularity in the last years. Many examples can be found both in literature and in the market, some of which are named as smart watches, smart rings and fitness trackers. Smart eyewear devices have also gained considerable attention from the product manufacturers, with some products already available and some second versions prepared for market [1-5]. Currently, the connectivity of these devices is limited to Wi-Fi 802.11b/g and Bluetooth and the user can only connect to a hot-spot or a paired smartphone. It could be foreseen that these devices may someday be integrated into the wireless cellular network which necessitates the integration of appropriate antennas. Concerning LTE-A (Long Term Evolution) or 4G operation, the internal antenna has to cover 700-960 MHz as the Low-Band (LB) and 1700-2700 MHz as the High-Band (HB). The authors have previously demonstrated in [6] that it is possible to achieve such frequency coverage using a capacitive coupling element (CE) type antenna in an eyewear device. CE type antennas are non-resonant structures used to excite the proper wavemodes on the system ground plane. This way, the low-quality factor of the ground plane is utilized to get higher bandwidth potential which could be impossible to achieve if using an electrically small resonant antenna. This antenna-structure is then tuned to the intended frequency band using a matching network. Some examples of coupling element type antennas can be found in [7-11].

A key challenge for the design of a smartphone antenna is the sensitivity of the antenna performance with respect to the environment changes. For example, it is widely known that dielectric detuning severely affects the reflection coefficient band coverage of the antenna of the smartphone when the user's hand and/or head comes closer to the antenna. This dielectric detuning effect is generally observed in the form of antenna bandwidth shifts to lower frequencies and the appearance of reflection coefficient peaks in the middle of the band of interest depending on the antenna type. Therefore, the user effects on smartphone antennas have been examined in the literature by several groups [11-13].

The antennas we proposed in [6] consist of CE type antennas with dual-band behavior: 700-960 MHz and 1700-2700 MHz. In order to mitigate any effects that may come from the user (here referring mostly to user's hand since the user's head is a part of the default scenario), a different and completely novel design concept targeting 4G coverage for eyewear devices is designed. The main design target is to achieve a wideband, complete coverage of the 700-2700 MHz interval (118 % relative bandwidth), so that the reflection coefficient level (-6 dB) is maintained despite the user's proximity and possibly versus different users having each slightly different permittivity characteristics. This presents significant design challenges over and above those faced in [6].

Section II introduces the simulation environment together with the design and optimization of the antenna in the default use-case (with user's head). A comparison of simulations and measurements of the reflection coefficient, total efficiency and radiation patterns taking into account the user's head is also presented in this section. The effect of the user's hand and the antenna performance in free space is discussed in Section III. Specific absorption rate (SAR) simulations and measurements are given in Section IV. Finally, some conclusions are presented in Section V.

Manuscript received June 2016.

A. Cihangir, C. Luxey are with EpOC, Université Nice Sophia Antipolis, Valbonne, France (phone: +33-(0)4-93-95-51-88; fax: +33-(0)4-93-95-51-89; e-mail: cyril.luxey@unice.fr)

F. Gianesello is with STMicroelectronics, Crolles, France.

C. Panagamuwa and W. Whittow are with the Wireless Communications Research Group, Wolfson School of Mechanical, Electrical and Manufacturing Engineering, Loughborough University, Loughborough LE11 3TU, U.K. (e-mail: C.J.Panagamuwa@lboro.ac.uk; w.g.whittow@lboro.ac.uk).

## II. Broadband Antenna Design

The antenna was optimized for the scenario involving the head of the user together with a dielectric frame that houses the printed circuit board (PCB) of the antenna (Fig. 1). The Specific Anthropomorphic Mannequin (SAM) head has been used for both simulation and measurements. This scenario emulates a use-case where the user is wearing the eyewear. The eyewear frame was designed and optimized to fit over the SAM head in EMPIRE XCcel electromagnetic software. 3D-printing fast prototyping technology was selected for fabrication. Acrylonitrile-Butadiene-Styrene (ABS-M30) material was selected for the final eyewear frame transferred to the printer as an .STL file from EMPIRE XCcel. In order to ensure accurate simulations, the dielectric properties of the ABS-M30 material were measured using a Fabry-Perot resonator: $\varepsilon_r = 2.97$ and $\tan\delta = 0.029$. The parts of the frame on the right side of the head acts as a dielectric casing for the PCB (casing length is 168 mm, height is 19 mm and width is 6.8 mm). There is a hollow region inside the casing for the placement of the antenna PCB, having a width of 4.8 mm, leaving dielectric walls of 1mm thickness on each side (Fig. 1). For the head tissue, liquid properties at 1450 MHz were used in simulations as a mid-value of the target band: $\varepsilon_r = 40.5$ and $\tan\delta = 0.367$.

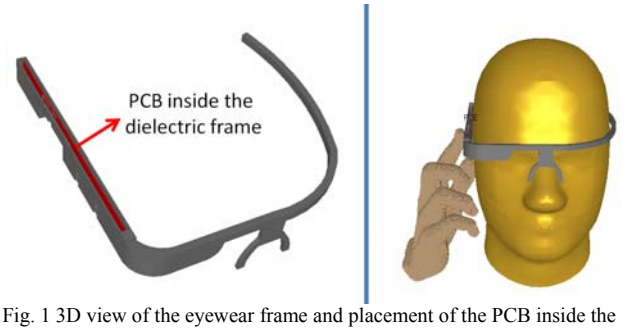


Fig. 1 3D view of the eyewear frame and placement of the PCB inside the frame (left side). Position of user's hand and fingers (right side).

The antenna is an L-shaped CE positioned behind the user's ear (Fig. 2). This CE is printed on the outer side of the PCB, formed by a 0.8 mm thick FR4 substrate ($\varepsilon_r = 4.4$ and $\tan\delta = 0.02$). The ground plane is printed on the other side of the PCB, towards the head. To optimize the length of the CE and ground clearance, a parametric study was performed simulating the CE without any matching network (MN). The bandwidth potential (BP) improves as the CE length is increased (S-parameters from full electromagnetic wave simulations are used in Optenni Lab software [14] for BP calculation). For each frequency point, the software generates a MN of two lumped components and records the frequency interval under a pre-defined reflection coefficient threshold value (-6 dB chosen here). Here, 2000 MHz of BP centered at 1700 MHz is needed to cover the 700-2700 MHz frequency interval. The highest BP can be achieved when the CE has a length of 15 mm, which is the maximum PCB width. A similar result is found for the effect of ground clearance: larger ground clearance gives higher BP. For practical reasons, the ground clearance region was limited to 10 mm. The final optimized layout of the antenna can be seen in Fig. 3. On the inner side of the PCB (looking towards the user's head), the metalized ground plane is etched and the battery of the device is modelled as a rectangular metallization behind the ear of the user. The simulated input impedance of the antenna without any MN can be seen in Fig. 4, plotted between 700-2700 MHz (dashed curve).

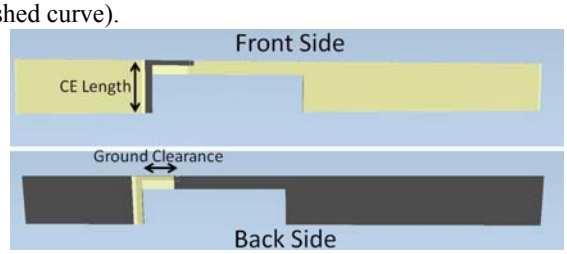


Fig. 2 CE parameters used for optimization (PCB of the eyewear device)

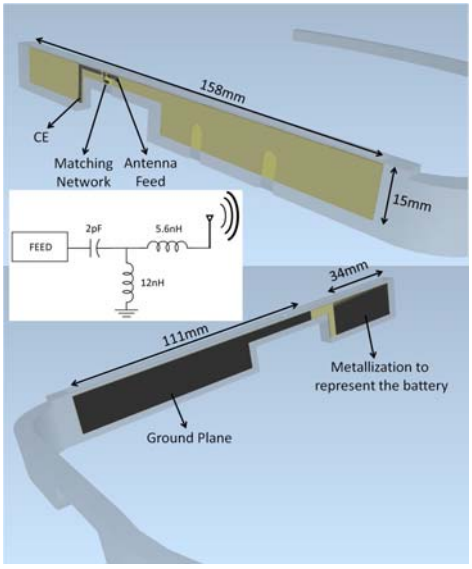


Fig. 3 Model of the optimized antenna and its matching network

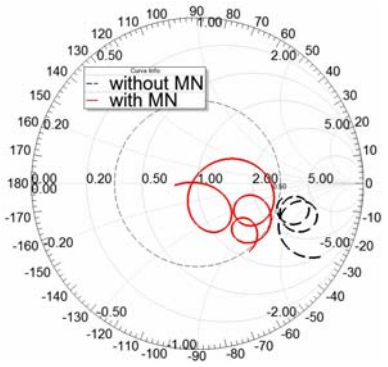


Fig. 4 Simulated input impedance of the optimized antenna with/without a 2-element MN (700-2700 MHz)

Using this simulated input impedance without any MN, the BP of the antenna was computed (Fig. 5, black solid and dashed lines). The matched antenna has a BP larger than 260 MHz at 830 MHz which is necessary to cover 700-960 MHz and higher than 1000 MHz at 2200 MHz to cover 1700-2700 MHz. In order to negate the detuning effect of the hand, the BP was further increased by adding a third matching component making it a single band antenna with continuous coverage from 700 to 2700 MHz (reflection coefficient below -6 dB). Fig. 5 presents the achievable BP for a 2-element and a

3-element MN. The BP target level required to continuously cover 700-2700 MHz is given by the dotted red line. As expected, the BP with a 3-element MN is higher and it is sufficient to cover the target band continuously.

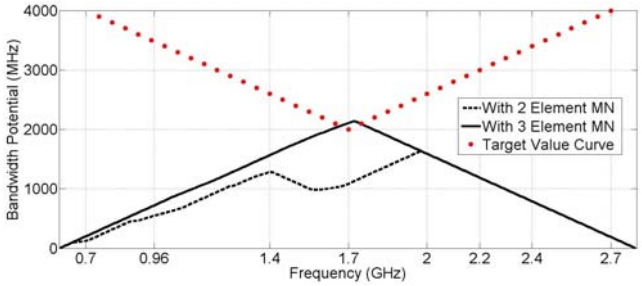


Fig. 5 Bandwidth Potential of optimized antenna for 2-element and 3-element matching networks with -6 dB reflection coefficient threshold

The simulated input impedance of the antenna with 3-elements MN can be seen in the Smith Chart in Fig. 4. The corresponding reflection coefficient at the input port of the antenna is given in Fig. 6. It can be seen that the target band of 700-2700 MHz can be covered continuously with a reflection coefficient below -6 dB.

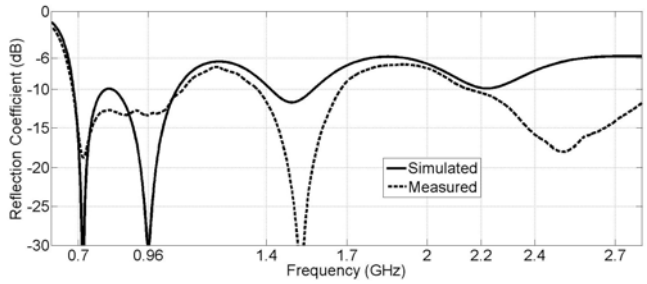


Fig. 6 Simulated and measured reflection coefficient of the optimized antenna with frame on the SAM head

The measured reflection coefficient with this frame and the fabricated PCB is presented in Fig. 6. Good agreement with simulated results is obtained. The total efficiency and radiation pattern measurements were performed in a Satimo Starlab station with the SAM head phantom. Fig. 7 shows good agreement between simulated and measured total efficiency, where the measured efficiency ranges from 7 % to 9 % (around 700 MHz) [15] and 9 to 23 % in the high band. The simulated and measured 2D gain patterns are not presented here for sake of brevity. As expected, the radiation in the direction of the head is weak due its lossy characteristics (absorption in the head tissue). The radiation is always maximum in the direction away from the head in the horizontal plane. The horizontal polarization is always more dominant than the vertical polarization by up to approximately 9 dB in the LB and 6 dB in the HB, because of the main horizontal currents flowing along the length of the PCB. Table 1 presents the simulated and measured maximum gain values for four different frequency points. A fair compliance can generally be observed between simulation and measurement.

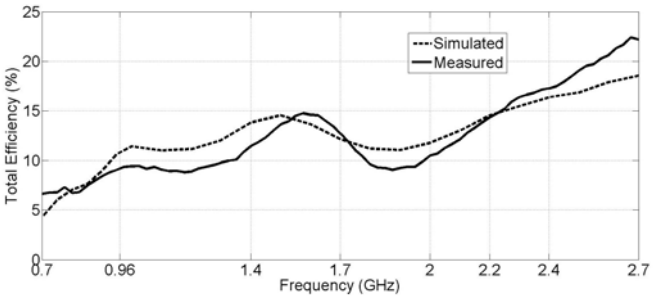


Fig. 7 Simulated and measured total efficiency of the optimized antenna with head and frame

TABLE 1 SIMULATED AND MEASURED MAXIMUM GAIN OF THE ANTENNA

| | 700 MHz | 950 MHz | 2200 MHz | 2700 MHz |
|---|---|---|---|---|
| Simulated | -7.45 dBi | -3.96 dBi | -0.79 dBi | 0.75 dBi |
| Measured | -6.27 dBi | -3.75 dBi | -1.78 dBi | 1.66 dBi |

## III. MEASUREMENTS IN DIFFERENT USAGE CASES

As previously mentioned, three realistic use-cases are targeted for the smart eyewear devices: i) "free space" condition where the eyewear is not worn by the user but might need to be operational for incoming calls (ABS frame with integrated antenna is placed horizontally on a foam support); ii) general use-case "with SAM head" configuration (which was used in Section II); iii) "with SAM head and phantom hand" which emulates the case in which the user uses the touchpad on the side of the device. A real human male head configuration was also tested for S-Parameter measurements. The measured reflection coefficients in all the different use-cases can be seen in Fig. 8. As expected, the reflection coefficient performance is slightly worse in free space condition when compared to the "with head" case, because of the lossy nature of the head and also since the MN was optimized with the presence of this SAM head. The "with head" and "with head and hand" measurements have a good agreement suggesting minimum effect from the phantom hand. The measured reflection coefficient of the antenna when it is worn by different real human users is presented in Fig. 9. The targeted matching level is accomplished despite some resonance shifts observed for different users (which might reflect different distances between the antenna and the heads, thus different loading characteristics). So, in all different use-cases (and thus different environments), the -6 dB reflection coefficient criterion is preserved in the 700-960 and 1700-2700 MHz bands (-5.9 dB for the entire 700-2700 MHz band), which was the main goal of this work: targeting an ultra-broadband antenna robust to user's detuning. The measured total efficiency of the three use-cases was highest for "free space" as expected, ranging from 43 to 68 % in the target bands (Fig. 10). The effect of the hand versus the total efficiency can be seen in the same figure, decreasing the efficiency by 3-4 % compared to the "with head" use-case (but still ranging from 7 to 9 % in LB and 7 to 19 % at the HB). To sum up, the antenna design seems to be appropriate for eyewear communications in terms of matching, total efficiency and radiation patterns. It also shows detuning robustness due to various operating environments.

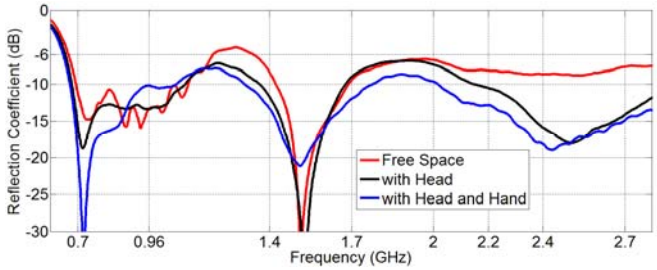


Fig. 8 Measured reflection coefficient for different use cases

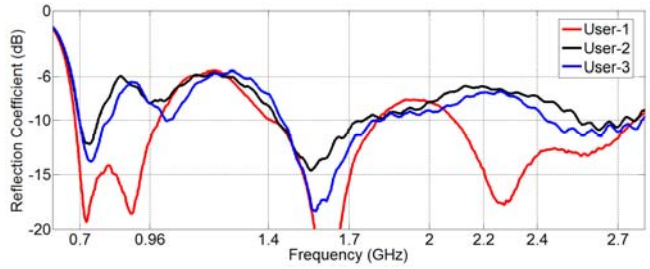


Fig. 9 Measured reflection coefficients with real users

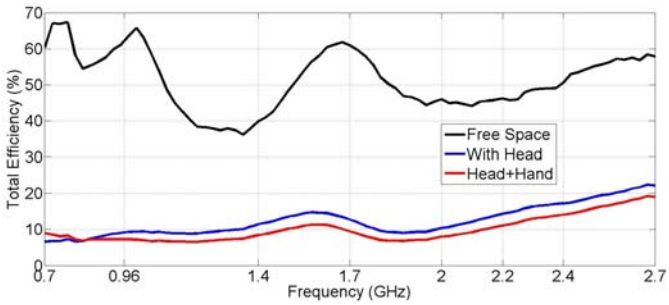


Fig. 10 Measured total efficiency for different use cases

## IV. SAR Simulations and Measurements

RF Power absorbed by a unit mass of tissue in W/kg is referred to as SAR and is the internationally recognized dosimetric parameter for testing wireless devices. In Europe, the SAR limit in the head is 2 W/kg averaged over 10 g for 6 minutes. In the USA, it is 1.6 W/kg averaged over 1 g for 30 minutes. The 1 g and 10 g spatially averaged SAR was simulated in EMPIRE XCcel using the SAM head phantom. Measurements were carried out using a Dosimetric and near-field Assessment System (DASY4). SAR measurements were taken with CW RF input signals at 900 and 1900 MHz (Table 2). All results are normalized to 0.25 W accepted power after accounting for the port mismatch losses ($S_{11}$). In all cases, simulated and measured SAR values exceed the international limits. This is partially due to the fact that the total antenna efficiency is double the typical values with generic smartphones with head and hand. In this study, the antenna is also much closer to the phantom head compared to a smartphone that normally rests against the pinna and has the antenna placed on the side of the case away from the head.

TABLE 2 SIMULATED AND MEASURED 1 G AND 10 G SAR (W/KG) FOR OPTIMIZED ANTENNAS. POWER NORMALIZED TO 0.25W ACCEPTED POWER

| Frequency (MHz) | 1 g SAR | 10 g SAR |
|---|---|---|
| 900 (sim.) | 5.4 | 3.0 |
| 900 (meas.) | 4.1 | 2.4 |
| 1900 (sim.) | 11.8 | 5.3 |
| 1900 (meas.) | 8.6 | 4.1 |

## V. Conclusion

An antenna for 4G eyewear device was designed. A realistic ABS frame which fits the SAM head was designed and manufactured using 3D-printing technology. The antenna is of CE type, placed behind the user's ear. In order to make the design robust to detuning due to changing environments, the antenna was designed to continuously cover 700-2700 MHz (118% bandwidth). Simulations and measurements demonstrated the CE approach is definitely the best viable approach for this ultra-broadband coverage given that a resonant structure would not be able to cover the whole 700-2700 MHz band. SAR simulation and measurements values at 900 and 1900 MHz were found to be higher than the US and Europe SAR standards which would require the output power to be reduced to comply with the regulations. This is partially due to the fact that the total efficiency is double the typical values with generic smartphones with head and hand.

## References

[1] "Google Glass," Available at: http://www.google.com/glass/start/
[2] "M100 Smart Glass," Available at: http://www.vuzix.com/UKSITE/consumer/products_m100.html
[3] "RECON Jet," Available at: http://www.reconinstruments.com/products/jet/
[4] "Olympus MEG4.0," Available at: http://www.olympus.co.jp/jp/news/2012b/nr120705meg40j.jsp
[5] "Google Glass Gets a Second Life in the ER," Available at: http://spectrum.ieee.org/the-human-os/biomedical/devices/google-glass-gets-a-second-life-in-the-er
[6] A. Cihangir, W.G. Whittow, C.J. Panagamuwa, F. Ferrero, G. Jacquemod, F. Gianesello, C. Luxey, "Feasibility Study of 4G Cellular Antennas for Eyewear Communicating Devices," IEEE Antennas and Wireless Propagation Letters, vol. 12, pp. 1704-1707, 2013.
[7] P. Vainikainen, J. Ollikainen, O. Kivekas, I. Kelander, "Resonator-based analysis of the combination of mobile handset antenna and chassis," IEEE Trans. on Ant. & Prop., vol. 50, no. 10, pp. 1433-1444, Oct. 2002
[8] J. Villanen, J. Ollikainen, O. Kivekas, P. Vainikainen, "Coupling element based mobile terminal antenna structures," IEEE Transactions on Antennas and Propagation, vol.54, no.7, pp. 2142-2153, July 2006.
[9] J. Villanen, C. Icheln, P. Vainikainen, "A coupling element-based quad-band antenna structure for mobile terminals," Microwave and Optical Technology Letters, vol. 49, no. 6, pp. 1277-1282, June 2007.
[10] A. Andujar, J. Anguera, C. Puente, "Ground Plane Boosters as a Compact Antenna Technology for Wireless Handheld Devices," IEEE Trans. on Antennas & Propag., vol. 59, no. 5, pp. 1668-1677, May 2011.
[11] R. Valkonen, J. Ilvonen, P. Vainikainen, "Naturally non-selective handset antennas with good robustness against impedance mistuning," 6th European Conference on Antennas and Propagation 2012 (EuCAP 2012), pp.796-800, 26-30th March 2012.
[12] J. Ilvonen, R. Valkonen, J. Holopainen, O. Kivekas, P. Vainikainen, "Reducing the interaction between user and mobile terminal antenna based on antenna shielding," 6th EuCAP 2012, 26-30 March 2012.
[13] M. Pelosi, O. Franek, G. F. Pedersen, M. Knudsen, "User's Impact on PIFA Antennas in Mobile Phones," 69th VTC Spring, 26-29 April 2009.
[14] Optenni Lab, Information Available at: http://www.optenni.com/optenni-lab/
[15] P. Ikonen, J. Ella, E. Schmidhammer, P. Tikka, P. Ramachadran, P. Annamaa, "Multi-feed RF front-ends and cellular antennas for next generation smartphones," Available via. http://www.pulseelectronics.com/download/3755/indie_technical_article/pdf